Novel reactions catalysed by antibodies

Beatrice Golinelli-Pimpaneau

Commentary
Novel reactions catalysed by antibodies

Béatrice Golinelli-Pimpaneau

New structural data on nonhydrolytic antibody catalysts gained over the past two years confirm that antibodies elicited against transition state analogues function by differential stabilisation of the transition-state over the ground state through electrostatic, van der Waals, cation–π and hydrogen-bonding interactions. The lack of chemical catalysis correlates with the low catalytic efficiency. Novel strategies that precisely position a key functional residue in the antibody catalyst combining site have therefore emerged, as demonstrated by crystallographic studies. Whereas antibodies with a bulky residue at position H100c of hypervariable loop H3 adopt different cavity shapes, other antibodies share a common deep combining site. This structural restriction might reflect the use of similar hydrophobic haptens to generate the antibody; novel hapten design or new immunisation strategies may, in the future, lead to more structurally diversified active sites.

Addresses
Laboratoire d'Enzymologie et Biochimie Structurales, CNRS Bât 34, 1 avenue de la Terrasse, 91198 Gif-sur-Yvette Cedex, France; e-mail: beatrice.golinelli@lebs.cnrs-gif.fr

Current Opinion in Structural Biology 2000, **10**:697–708

0959-440X/00/$ – see front matter

Abbreviations

CDR	complementarity-determining region
PDB	Protein Data Bank
V_H	heavy chain variable domain
V_L	light chain variable domain

Introduction

Since 1986, it has been shown that antibodies generated by immunisation with appropriate transition-state analogues are able to catalyse a variety of chemical transformations [1,2]. An examination of structural data concerning catalytic antibodies, combined with biochemical studies, elucidates their mechanisms, as well as provides insight into enhancing their catalytic efficiencies. This is necessary for these tailor-made catalysts to be used in practical applications as biochemical reagents, chemical process catalysts or therapeutics.

Previously published reviews on the structures of catalytic antibodies focused mainly on hydrolytic reactions [3–6]. Crystal structures of antibodies with novel nonhydrolytic activities have emerged these past two years (Table 1, Figure 1), including examples of antibody-catalysed disfavoured reactions, in which the binding energy serves to drive the chemical reaction in an otherwise inaccessible direction. Affinity maturation introduces somatic mutations into the antibody that increase binding affinity to the hapten. [A hapten is a small molecule that is not immunogenic by itself; however, when this molecule is conjugated to a carrier protein, it has the ability to stimulate the formation of antibodies highly specific and complementary to its structure.] The structural basis for the effect of these mutations on the catalytic rate was established in two cases by comparing the mature antibody and its germline counterpart. Structures have also validated strategies different from the classical transition-state analogue approach that aim to generate chemically reactive residues in the combining site of antibodies.

This commentary first summarises the details about the catalytic mechanisms that have been provided by X-ray structures of antibody–hapten complexes. Then, the antibody catalytic pockets are compared through superposition of their coordinates to gain insight into the diversity of modes of binding of the hapten to the recombinant site and to evaluate the key positions of the complementarity-determining regions (CDRs) that are responsible for the catalytic activity.

Transition-state analogue approach

The design of an antibody catalyst most often relies on the use of a hapten that is sterically and electronically similar to the transition state (or high-energy intermediate) of the reaction to be catalysed. The concept relies on the higher affinity of the catalyst for the transition state of the reaction compared to that for the substrate. It has been successfully applied to reactions in which the transition state differs considerably from the ground state and has been validated by the structures of esterolytic antibodies [3,5] and, recently, of antibodies catalysing porphyrin metallation, unimolecular cyclisations and pericyclic rearrangements (Table 1).

Metal chelatase: catalysis by distortion

Metal chelatase antibody 7G12 utilises binding energy to induce geometric strain in the porphyrin substrate **1** (Figure 1a) [7]. The antigen-binding site lies at the interface of the heavy and light chain variable domains (V_H and V_L, respectively). Binding of the distorted conformation of the transition-state analogue hapten **3** is carried out by hydrophobic packing interactions with the antibody (Figure 2a). This fixes the position of pyrrole ring B, whereas pyrrole ring A, which is not held in position by V_H, can be activated for distortion. Analysis of the sequence of the germline antibody, coupled to mutagenesis, shows that the somatic mutation at position H100c (serine to methionine) increases the affinity of the antibody for the distorted transition state and therefore suggests that MetH100c, which occupies the floor of the binding pocket, is a key residue in the strain mechanism of antibody 7G12.

Table 1

Kinetic parameters and some structural characteristics of nonhydrolytic antibody catalysts*.

Antibody	Activity	Kinetic parameters			Structural features		
		k_{cat}/K_m (M^{-1} min^{-1})	k_{cat} (min^{-1})	k_{cat}/k_{non}	Resolution (Å)	PDB code	References
7G12	Porphyrin metallation†	2.7	0.4	1700	2.4	3fct	[7]
5C8	*endo* cyclisation of an epoxyalcohol‡	2.8×10^3	1.7	ND§	2.0	25c8	[8]
19A4	Polyene cyclisation	66	0.021	$>2 \times 10^3$	2.7	1cf8	[10]
1F7	Chorismate mutase	1.4×10^5	0.07	190	3.0	1fig	[12]
AZ-28	oxy-Cope rearrangement	311	0.023	5300	2.6	1axs	[15]
Germline		1.1×10^4	0.8	1.63×10^5	2.0	1d5c	[16]
39-A11	Diels–Alderase	$3.5 \times 10^{4\#}$ $5.4 \times 10^{4\P}$	40.2	0.35 M	2.4	1a4k	[17]
Germline		$7.3 \times 10^{3\#}$ $2.3 \times 10^{4\P}$	10.2	0.09 M	2.1	1a4j	[17]
1E9	Diels–Alderase	$5.4 \times 10^{3\#}$ 450¶	13	10^3 M	1.9	1c1e	[19]
13G5	*exo* Diels–Alderase‡	0.44# 0.12¶	1.2×10^{-3}	6.9 M	1.95	1a3l	[18]
28B4	Periodate-dependent oxidation of sulfide	1.1×10^7	492	9.65 M	1.9	1kel	[22]
33F12**	Aldolase		10^{-3} –5	10^5 –10^7	2.15	1axt	[25]
	Allylic rearrangement	230	0.54	1.2×10^3			
4B2	Allylic rearrangement	1.2	1.6×10^{-3}	1500	1.87	1f3d	[30]
	Kemp elimination	1.3	630	6.3×10^3			

*A previously published review [4] covers the chorismate mutase and sulfide oxidase antibody catalysts, which are only briefly discussed in the text (see also Update). †The kinetic constants are for copper metallation. ‡Disfavoured reaction. §Not determined: the disfavoured *endo* product is negligible in the uncatalysed reaction. #Diene. ¶Dienophile. **Unliganded structure.

In addition, AspH100b has been shown by mutagenesis to be essential for catalytic activity; its carboxylate is positioned 1.9 Å from the centre of the porphyrin ring. This indicates that it could facilitate metal complexation either by acting as a general base to deprotonate the nitrogen of the porphyrin substrate or by forming a metal–oxygen bond. This would explain that the catalytic efficiency of 7G12 approaches that of the enzyme ferrochelatase.

Unimolecular cyclisation

Antibodies that catalyse unimolecular cyclisation use binding energy to constrain the acyclic substrate, leading to an appropriate conformation for concerted cyclisation. Antibody 5C8 catalyses the one-step 6-*endo* cyclisation of epoxyalcohol **4**, a reaction that is strongly disfavoured in solution, with high regioselectivity and enantioselectivity (Figure 1b) [8]. The catalytic effect appears to come from electronic stabilisation and, possibly, general acid/base catalysis. The antibody selectively stabilises the higher energy six-membered transition state by electrostatic stabilisation of the higher partial positive charge that develops at the epoxide carbon atom. Although some charge stabilisation may be achieved by the distant residue AspH101, the main charge stabilisation probably comes from cation–π interactions, as numerous aromatic or histidine residues border the antibody combining site (Figure 2b). In addition, HisL89 and AspH95 could act as a base/acid dyad, respectively, to deprotonate the alcohol group and increase its nucleophilicity, or to protonate the epoxide oxygen atom in order to make it a better leaving group and facilitate epoxide opening. This interpretation is supported by the structure of antibody 5C8 complexed with an *N*-oxide analogue of hapten **6**, in which the *N*-oxide oxygen makes an hydrogen bond to AspH95 [8].

Polyene cyclisation is another class of unimolecular rearrangement reaction; it is among the most demanding reactions to have been catalysed by antibodies and is of great interest to gain access to steroidal carbon frameworks. Although the uncatalysed cationic reactions result in a mixture of elimination and addition products, they can be re-routed via antibody catalysis to yield predominantly one product [9]. Antibody 19A4 catalyses a multistep cationic cyclisation (Figure 1c) [10]. After binding the linear polyene substrate **7** in a productive chair–chair conformation, it has been proposed that the carbocation cyclisation cascade is initiated by AsnH35, which might help trigger departure of the sulfonate leaving group by hydrogen bonding (Figure 2c). This assumes that the sulfonate leaving group would occupy the same position as the nitroxide oxygen of hapten **9**; this needs further crystallographic evidence. The antibody mainly utilises aromatic amino acid residues for the stabilisation of either the positive charge developing on the substrate C1 atom or the C5 and C9 high-energy carbocationic intermediates. These cation–π interactions control the stereochemistry of the two-step cyclisation, as indicated by the formation of only the *trans* decaline skeleton **8**, but there is no catalytic base to direct the regiochemistry of the final proton elimination step to yield one exclusive olefin.

Unimolecular pericyclic rearrangements

The transition-state analogue approach has been particularly useful as a source of catalysts for transformations such

Figure 1

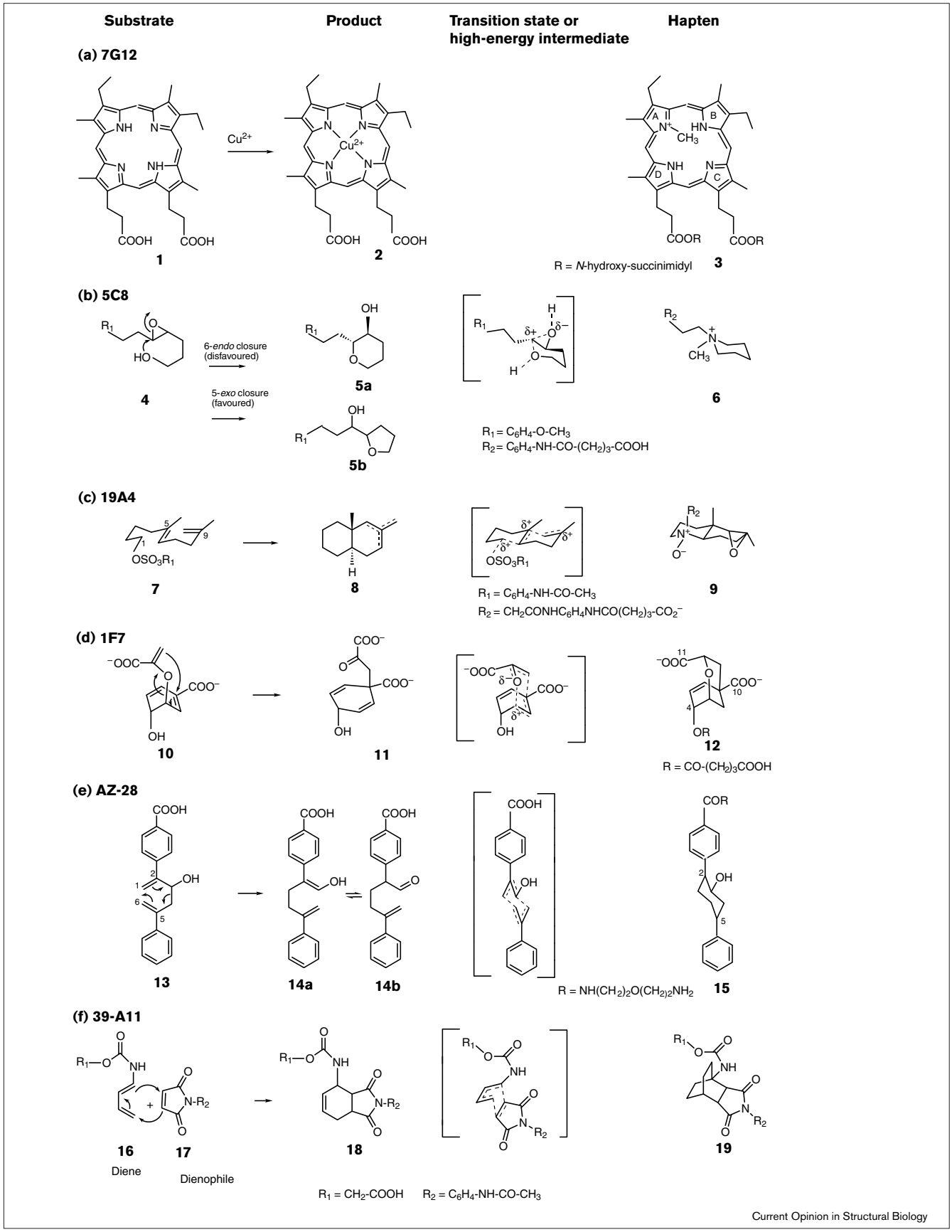

Current Opinion in Structural Biology

Figure 1 continued

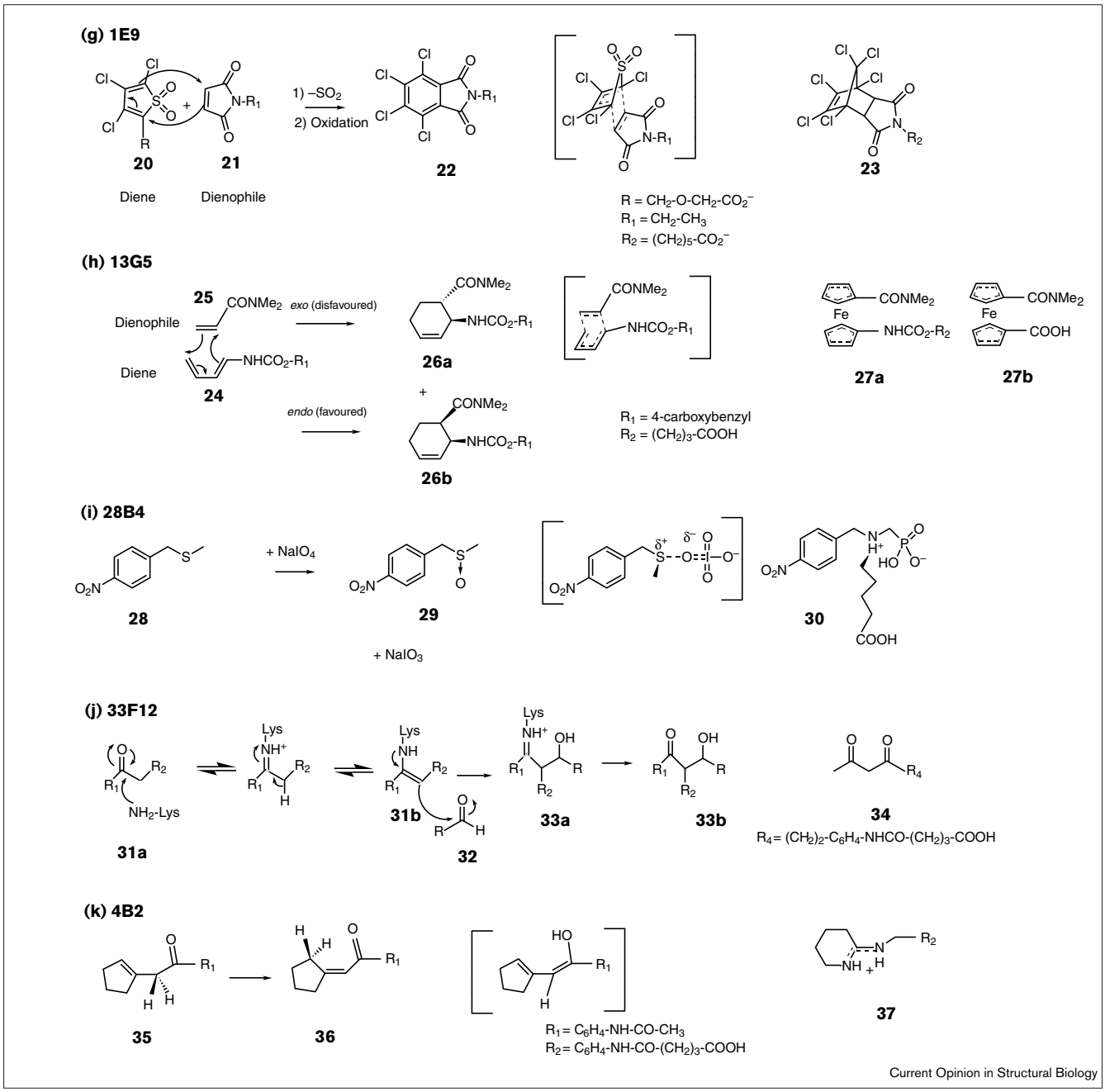

as cycloadditions, which are characterised by a highly ordered transition state. As there are relatively few examples of enzyme-catalysed pericyclic processes and in view of their synthetic utility [11], these reactions remain a major focus for the catalytic antibody field, as illustrated by new structural reports documenting antibody-catalysed pericyclic reactions (Table 1).

Unimolecular pericyclic rearrangements involve a conformationally flexible substrate, which evolves towards a chair-like transition state in which the 4π and 2σ orbitals partially overlap in a cyclic array. The first structure of a complex between an antibody catalyst and its hapten involved the chorismate mutase antibody 1F7 (Figure 1d) [12]. The Claisen rearrangement is a well-suited goal for antibody catalysis, as the enzyme-catalysed reaction does not require any functional group to form a covalent intermediate with the substrate or to participate in general acid/base catalysis [13,14]. Antibody 1F7 organises the substrate into the chair-like reactive conformation by forming van der Waals interactions and a network of hydrogen bonds with the carboxylates. The natural

Figure 1 legend

Schemes of the reactions catalysed by the structurally characterised antibodies. **(a)** 7G12 catalyses metal insertion into the mesoporphyrin ring of **1**. As the enzyme-catalysed reaction is thought to result from strain of the planar porphyrin ring substrate toward a distorted transition state, this antibody was induced by *N*-alkylmesoporphyrin hapten **3**, which adopts a distorted geometry mimicking that of the transition state. **(b)** 5C8 catalyses the disfavoured intramolecular 6-*endo* ring closure of *trans*-epoxyalcohol **4** to yield the six-membered product **5a**, whereas the uncatalysed reaction gives the five-membered product **5b**. 5C8 was generated against *N*-methyl piperidinium hapten **6**, which possesses both a ring conformation that approximates the required geometry during 6-*endo* ring closure and a positive charge mimicking that which develops at the epoxide carbon atom during the transition state. No feature of the hapten mimics the developing negative charge at the epoxide oxygen atom. **(c)** 19A4 catalyses the cationic cyclisation of polyene **7** to form the bicyclic isomeric products **8**. The half-chair conformation of the second six-membered ring in hapten **9** was expected to induce an antibody combining site that enforces the appropriate conformation of substrate **7**. The positively charged nitrogen atom of *N*-oxide hapten **9** mimics the developing positive charge on C1 of substrate **7**. **(d)** 1F7 catalyses the unimolecular Claisen rearrangement of chorismate **10** to prephenate **11**. It was induced against hapten **12**, which mimics the chair-like geometry, but not the highly dipolar nature, of the transition state. **(e)** AZ-28 catalyses the oxy-Cope rearrangement of hexadiene **13**. Rapid conversion of the enol group in product **14a** leads to the aldehyde **14b**, which is trapped *in situ* with hydroxylamine. AZ-28 was obtained through immunisation with hapten **15**, a chair-like analogue of the preferred chair transition state of the rearrangement. **(f)** 39-A11 catalyses the Diels–Alder reaction of diene **16** and dienophile **17** to form bicyclic product **18**. 39-A11 was generated against bicyclic hapten **19**, a mimic of the boat-like transition state of the reaction. The conformation of hapten **19** differs from that of the chair-like product, thereby preventing product inhibition. **(g)** The product of the cycloaddition of diene **20** and dienophile *N*-ethylmaleimide **21**, catalysed by 1E9, spontaneously extrudes SO_2 and oxidises to form aromatic product **22**, which is sufficiently different from the transition state that no product inhibition occurs. **(h)** 13G5 catalyses the Diels–Alder reaction between carbamate diene **24** and N,N-dimethylacrylamide **25** to give only the *exo* regioisomer **26a** in high enantiomeric excess. This reaction is disfavoured relative to the formation of the *endo* adduct **26b**. 13G5 was raised against ferrocene derivative **27a**, which, with its two pentagonal delocalised π-electron ring systems stacked upon each other, acts as a loose mimic of a very early boat-like transition state. 13G5 was crystallised in the presence of the more chemically stable ferrocene inhibitor **27b**. The ferrocenyl carboxylic acid of **27b** represents the carbamate of diene **24** and the ferrocenyl (dimethylamino)-carbonyl mimics the N,N dimethylacrylamide of dienophile **25**. **(i)** 28B4 catalyses the oxidation of sulfide **28** with periodate to form sulfoxide **29**. The ammonium and phosphonate of hapten **30**, respectively, mimic the positive and negative charges that develop on sulfur and periodate in the transition state. **(j)** 33F12 catalyses a large array of aldol condensations. The Schiff base formed between an active site lysine residue and various ketone substrates **31a** leads to the enamine **31b**. Addition of this enamine to different aldehydes **32** leads to the Schiff base **33a,** which is hydrolysed to give the β-hydroxyketone product **33b**. During the immunisation process, diketone hapten **34** can form a stable vinylogous amide by reaction with the reactive lysine sidechain. **(k)** 4B2 catalyses the isomerisation of β–γ unsaturated ketone **35** to α–β unsaturated ketone **36**. 4B2 was induced against hapten **37**, which possesses an amidinium function for the induction of a complementary charged residue in the antibody, at a location that allows it to act as a general base.

enzymes accelerate the rearrangement more efficiently because they provide more hydrogen-bonding and direct electrostatic interactions to constrain the conformation of the chorismate substrate. In addition, they destabilise the substrate by hydrogen bonding to the hydroxyl group and, unlike the antibody, possess a dipolar active site well suited to stabilise the dipolar transition state.

Antibody AZ-28 catalyses a related [3,3] sigmatropic rearrangement that has no natural counterpart, the oxy-Cope rearrangement of hexadiene **13**, through a combination of electronic and entropic effects (Figures 1e and 2d) [15]. Binding of the substrate in a chair-like conformation places the hexadiene in favourable orbital alignment. However, the two phenyl substituents of hapten **15** are rotated out of plane with respect to the cyclohexyl ring. This conformation of the transition state is catalytically unfavourable because of decreased π orbital overlap between the hexadiene system and the aryl substituents. A comparison of the X-ray structures of the germline and affinity-matured antibodies [16] has shown that the somatic mutation of SerL34 to AsnL34 decreases the flexibility of CDR loop H3 and leads to restricted substrate rotation around the C2 aryl bond and decreased orbital overlap. This explains why the rate enhancement of the mature antibody is, surprisingly, 30-fold lower than that of its germline precursor.

Diels–Alderases: bimolecular pericyclic reactions

The crystal structures of three antibody catalysts that accelerate a Diels–Alder reaction have been recently reported (Table 1) [17–19]. This reaction consists of the 1,4 cycloaddition of an alcene (or dienophile) to a diene, and yields cyclic compounds of great interest in synthetic organic chemistry. It is facilitated by the presence of electron-donating groups on the diene (donor) and electron-withdrawing functionalities on the dienophile (acceptor), and involves the stacking of the 4π and 2π orbitals to form a boat-shaped transition state. Two approaches have been used to generate antibodies capable of catalysing this reaction. The first uses rigid, bicyclic transition-state analogues **19** and **23** (Figure 1f,g), and the other uses a conformationally unrestricted ferrocene derivative, **27a** (Figure 1h).

The structure of 39-A11 suggests that the antibody binds the diene **16** and dienophile **17** in a reactive orientation and reduces their degrees of freedom (Figure 2e) [17]. Structural and functional studies of the germline precursor of 39-A11 suggest that a single somatic mutation, SerL91Val, is largely responsible for the 40-fold and four-fold increases in binding affinity and catalytic activity, respectively, of the mature antibody, probably because it partially eliminates a prominent cavity present around residues L91 and L89. The still low catalytic efficiency

Figure 2

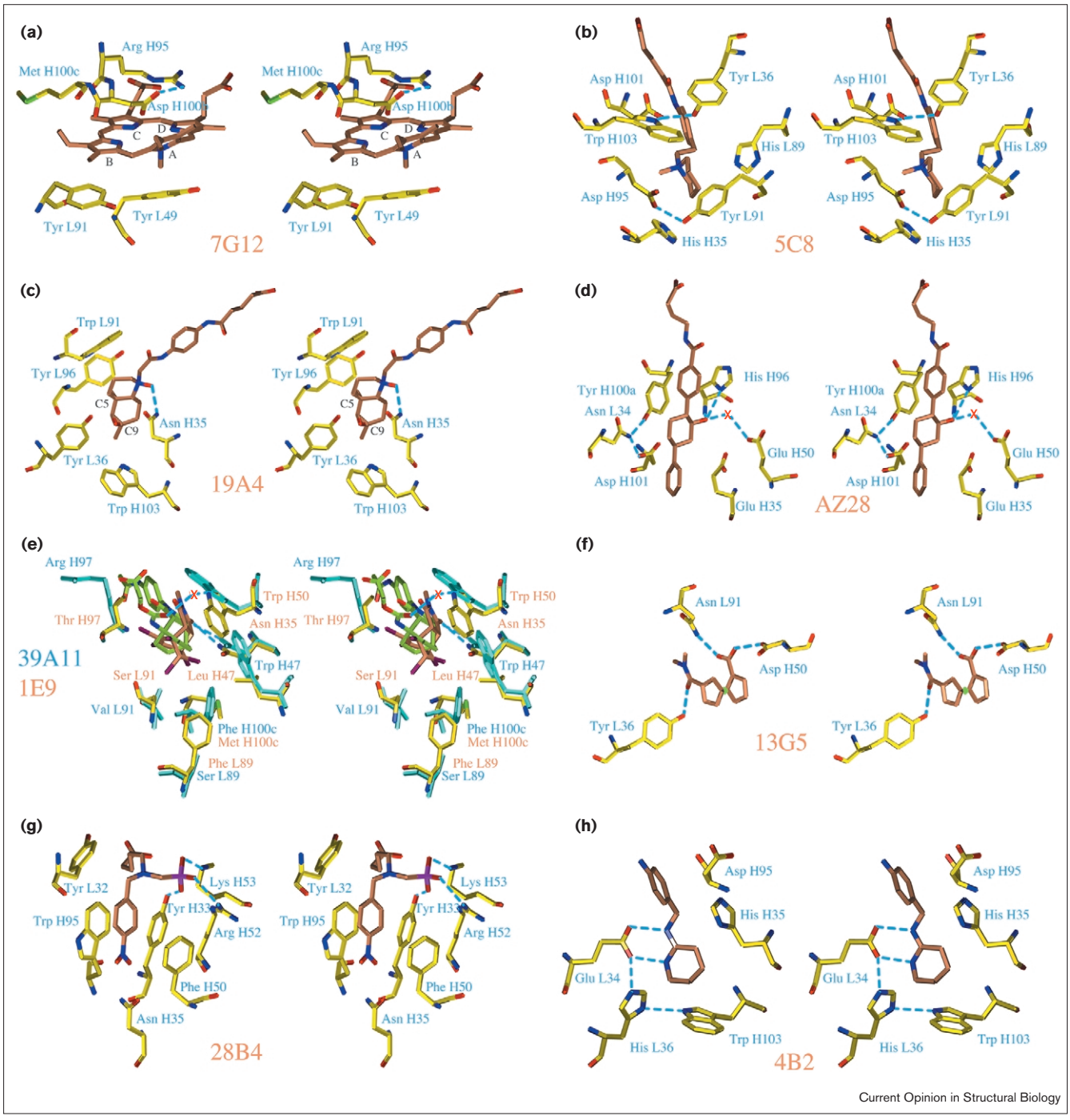

of 39-A11 can be attributed to the loose fit of its transition state with the binding site, which is exacerbated by the incorporation of an ethano bridge in the hapten **19** that occupies the bottom of the cavity and has no counterpart in the transition state (Figure 1f).

The crystal structure of 39-A11 has been compared to that of the related antibody 1E9, the most efficient Diels–Alder antibody catalyst known, which possesses a CDR H3 loop from a different origin, but of the same length and conformation (Figure 2e) [19]. Although the two antibodies stabilise the transition state using the same hydrogen bond between AsnH35 and the dienophile carbonyl, the higher efficiency of 1E9 comes from its almost perfect shape complementarity with its transition-state analogue hapten **23** (Figure 1g), which is mostly due to two somatic mutations. Although germline residue SerL91 is not mutated in 1E9, the nearby cavity that is

Figure 2 legend

Antibody–hapten complexes, showing the key antibody–ligand interactions that explain the catalytic activity. **(a)** 7G12. The antibody binds one isomer of porphyrin **3**, with pyrrole ring A *N*-methylated. Pyrrole rings A and B are buried at the bottom of the pocket, whereas pyrrole rings C and D, which bear the propionate substituents, are exposed to the solvent. Pyrrole rings B, C and D are coplanar and pyrrole ring A is distorted out of this plane by 42°. On one face of the porphyrin, TyrL49 and TyrL91 π-stack on pyrrole rings A and B, respectively, whereas on the other side, ArgH95, AspH100b and MetH100c from CDR H3 pack tightly against pyrrole rings B, C and D. The position of catalytic AspH100b is fixed by a hydrogen bond to ArgH95. **(b)** 5C8. The ammonium positive charge of hapten **6** is stabilised by cation–π interactions with TyrL91, HisL89, HisH35, TrpH103 and TyrL36, and by a weak electrostatic interaction with AspH101, which hydrogen bonds to TrpH103 and TyrL36. HisL89 is a putative base that deprotonates the alcohol oxygen of **4** and AspH95, which hydrogen bonds to TyrL91, is a putative acid that protonates its epoxide. The benzene moiety is positioned by π-stacking and hydrophobic interactions with HisL34 and ProH96, respectively (not shown). **(c)** 19A4. The *N*-oxide oxygen of hapten **9** hydrogen bonds to AsnH35 and its positively charged nitrogen is stabilised by cation–π interactions with TrpL91 and TyrL96. TrpL91 and TyrL36 probably stabilise the C5 carbocation intermediate and TyrL36 and TrpH103 probably stabilise the C9 carbocation intermediate. **(d)** AZ-28. AsnL34, which is positioned by hydrogen bonds to AspH101 and TyrH100a, restricts rotation around the C2 and C5 aryl bonds. The hydrogen bonds between residue L34 and H100a are 2.6 Å and 3.5 Å in the mature antibody–hapten and the germline antibody–hapten complexes, respectively. The 2-phenyl substituent π-stacks with TyrL91 (not shown), HisH96 and TyrH100a. The hydrogen bonds between the hydroxyl substituent and either residue HisH96 or the bridging water to GluH50 may enhance the rate of rearrangement by increasing the electron density on the hydroxyl substituent of the substrate. **(e)** Superposition of 39-A11 and 1E9. Water molecules are indicated as red crosses, hydrogen bonds as blue dashed lines. The atom colouring scheme is as follows: carbon atoms of the proteins in yellow (except for 39-A11 in cyan), carbon atoms of the ligand in orange (except for 39-A11 in spring green), oxygen in red, nitrogen in blue, sulfur in green, phosphorus in magenta, chloride in maroon. Although TrpH50 adopts different conformations in each antibody, it π-stacks, in both cases, with the succidimyl group of the hapten, which is isosteric with the maleimide ring of the dienophile substrate. In addition, the dienophile is fixed in close proximity to the diene through AsnH35, which donates a hydrogen bond to one of the succinimide carbonyl groups of haptens **19** or **23**, and, in 39-A11, through hydrophobic interactions between ArgH97 and the phenyl substituent of the hapten. The diene is oriented, in 39-A11, by a water-mediated hydrogen bond between its carbamate substituent and TrpH50, and, in 1E9, by tight contacts to the antibody, due to mutations of residues in positions L89, H47 and H100c. **(f)** 13G5. In the 13G5–**27b** complex, TyrL36, which is oriented by a hydrogen bond with the amide of GlyH100c (not shown), accepts a hydrogen bond from the amide carbonyl oxygen of the pentadienyl that mimics the dienophile. AsnL91 and AspH50, which are positioned by hydrogen bonds to HisL32 and TrpH47, respectively (not shown), hydrogen bond to the carboxylic acid that is equivalent of the carbamate of the diene. **(g)** 28B4. TyrL32 stabilises the positive charge of the ammonium of hapten **30** by a cation–π interaction. TyrH33, ArgH52 and LysH53 contact the oxygens of the phosphonate via hydrogen bonds and salt bridges. The phenyl ring of hapten **30** is sandwiched between the aromatic rings of TrpH95 and PheH50. **(h)** 4B2. GluL34, which is positioned by a hydrogen-bond network with HisL36 and TrpH103, makes an ionic interaction with the bidentate amidinium moiety of hapten **37**. GluL34 acts as a general base that abstracts the allylic proton. HisH35, which points its protonated nitrogen towards the hapten, or AspH95, after a conformational change, might act as an acid to protonate the carbonyl substrate or the enediolate intermediate.

present in the 39-A11 complex is filled in by residue L89, which is mutated from a serine to a phenylalanine in 1E9. The second mutation is the rare substitution of framework residue TrpH47 by leucine, which significantly deepens the active site by allowing the bulky contacting residue TrpH50 to rotate its indole ring and fill in the vacated space. In addition, residue H100c, which provides the hydrophobic floor of the binding pockets, is a phenylalanine in 39-A11, but a methionine in 1E9, which is much more adaptable to the ligand shape because of the flexibility of its sidechain. Finally, the 1E9 transition state is less polar than that of 39-A11, which catalyses a reaction involving a strong donor diene **16** and acceptor dienophile **17** (Figure 1f,g), and is better stabilised in the relatively nonpolar environment of the 1E9 binding site.

Antibody 13G5, which catalyses a disfavoured *exo* Diels–Alder reaction, was raised against transition-state analogue **27a**, a ferrocene derivative with cyclopentadienyl rings that are able to rotate freely in solution (Figure 1h) [18]. In the inhibitor (**27b**)–antibody complex, the ferrocene ring rotation is restricted because of steric constraints and specific interactions with the antibody. This validates the idea that the immune system can select one conformer of a flexible hapten that mimics one of the Diels–Alder transition states and, hence, can produce a specific Diels–Alderase. From the three hydrogen bonds that are made between **27b** and the antibody, a catalytic mechanism was proposed (Figure 2f). TyrL36 acts as a Lewis acid, activating the dienophile for nucleophilic attack. AspH50 would act as an electron donor that increases the nucleophilicity of the diene by hydrogen bonding to the NH of the diene carbamate. A third hydrogen bond, which also contributes to orient the substrates and control product formation and stereoselectivity, occurs between AsnL91 and the carbonyl oxygen of the carbamate. The three key residues have their sidechains fixed by an extensive hydrogen-bond network.

Antibodies that catalyse pericyclic reactions were designed to perform as an entropy trap and X-ray structures of Diels–Alderase antibody catalysts show how the catalyst controls the orientation of the two substrates to form the highly ordered transition state. However, the activation parameters of the two unimolecular rearrangements reveal that these antibodies function primarily by reducing the enthalpy of activation of the reaction [20,21]. The catalytic activity of antibodies catalysing pericyclic rearrangements can thus be explained partly by the presence of a hydrophobic microenvironment that serves to sequester the substrate(s) from aqueous solution and preorganise it (them) into a reactive complex, through a myriad of van der

Figure 3

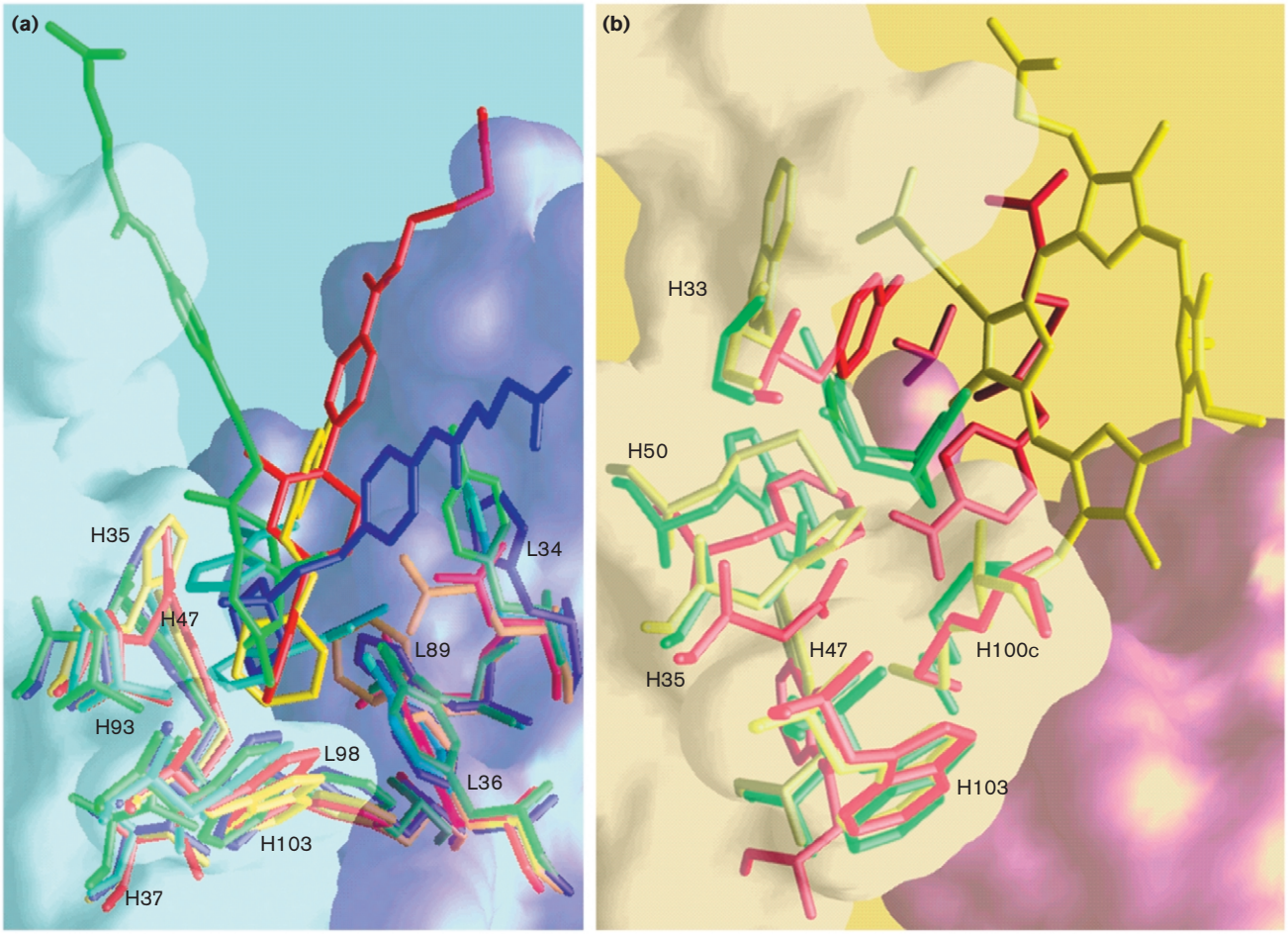

Comparison of the cavity shapes of the nonhydrolytic catalytic antibodies. **(a)** The cavity of antibodies that possess a CDR H3 loop with a small residue at position H100c. A section of the molecular surface of the combining site of antibody 4B2, omitting CDR H3 (in front), coloured in light blue for the heavy chain and light purple for the light chain, was obtained with the program GRASP. The α carbons of residues of the framework (L1–L25, L33–L49, L53–L90, L97–L107, H1–H25, H36–H51, H57–H93 and H103–H111) of antibodies 5C8, 19A4, AZ-28 and 13G5 have been superimposed on those of 4B2. The root mean squared deviations from 4B2 are 1.031 Å (5C8), 1.545 Å (19A4), 0.760 Å (AZ-28) and 1.072 Å (13G5). The hapten structures and the common residues of the combining site (L34, L36, L89, L98, H35, H37, H47, H93 and H103) are shown in stick representation, coloured in yellow (4B2), dark blue (5C8), green (19A4), red (AZ-28) and cyan (13G5). The hydrolytic antibodies CNJ206, 48G7 and 17E8, which possess, respectively, glycine, glycine and valine at position H100c, and D23, which has an extended conformation of its H3 C-terminal region that removes MetH100c from the bottom of the antigen-binding site, share the same combining site illustrated here [3,5,31]. The aryl (AZ-28, esterases), pentadienyl (13G5) or hydrophobic ring (5C8, 4B2, 19A4) substituents of the haptens maximise hydrophobic contacts with the antibody at the hydrophobic bottom of the cavity, which is made of conserved residues of the framework (TrpH103, PheL98, H93, TrpH47, Val/IleH37). This leads to a common shape for the bottom of the combining sites. The more variable residues in positions L34, L36, L89, H35 and L91 (not shown, for clarity) form the walls of the cavity and most often participate in catalysis. The terminal part of the haptens, which is linked to the carrier protein during the immunisation process, is solvent accessible and oriented differently in the various structures. **(b)** The cavity of antibody 7G12, as an example of an antibody with a bulky residue at position H100c of CDR H3. A section of the molecular surface of the combining site of 7G12 (omitting H95 and H100b, in front), coloured in light yellow for the heavy chain and pink for the light chain, is shown in the same orientation as (a). The α carbons of residues of the framework of antibodies 7G12, 1E9 and 28B4 have been superimposed on those of 4B2 [shown in (a)]. The root mean squared deviations are 1.044 Å (7G12), 1.476 Å (28B4) and 0.857 Å (1E9). The hapten structures and some common residues of the combining site (H33, H50, H100c), as well as H35, H47 and TrpH103, are shown in stick representation, coloured in yellow (7G12), green (1E9) and red (28B4). The atypical combining sites of hydrolytic antibodies 7C8 and 6D9 [compared with the cavity illustrated in (a)] [32] can be linked to the presence of a bulge phenylalanine at position H100c in both cases. Residue H100c, in each antibody, fills in the bottom of the cavity seen in (a), preventing contact of the haptens with buried TrpH103. The ligands bind at the upper part of the V_L–V_H interface and contact almost exclusively residues of the CDRs. There are, therefore, fewer common residues that make up the combining site (H33, H50, H95, H100a and H100c) and the cavity has different shapes and may be narrow, as illustrated here for 7G12.

Table 2

Sequence comparison of the active site residues of the structurally characterised nonhydrolytic catalytic antibodies*.

(a) Residue	Location	AZ-28	13G5	5C8	19A4	4B2
L32	CDR1	Tyr	His	Asn	Tyr	Tyr
L34	CDR1	**Asn**†	Tyr	His	Tyr	**Glu**
L36	FR2	Phe	**Tyr**	Tyr	**Tyr**	His
L49	FR2	Tyr	Tyr	Tyr	Tyr	Tyr
L89	CDR3	Leu	Ala	His	Leu	Phe
L91	CDR3	Tyr	**Asn**	Tyr	**Trp**	Gly
L96	CDR3	Tyr	Tyr	Tyr	**Tyr**	Tyr
L98	FR4	Phe	Phe	Phe	Phe	Phe
H33	CDR1	Trp	Trp	Tyr	Ala	Asn
H35	CDR1	Glu	Gly	His	**Asn**	His
H37	FR2	Val	Val	Val	Ile	Val
H47	FR2	Trp	Trp	Trp	Trp	Trp
H50	FR2	**Glu**	**Asp**	Gln	Tyr	Tyr
H93	FR3	Ala	Ala	Ala	Ala	Ala
H95	CDR3	Gly	Ala	Asp	Gly	Asp
H96	CDR3	**His**	Gly	Pro	Tyr	Tyr
H98	CDR3	Tyr	Tyr	Tyr	–	–
H100a	CDR3	Tyr	Thr	Gly	Gly	–
H100c	CDR3	Gly	Gly	Gly	Ser	Gly
H101	CDR3	Asp	Asp	Asp	Asp	Val
H103	FR4	Trp	Trp	Trp	**Trp**	**Trp**

(b) Residue	Location	1F7	39A11	1E9	7G12	28B4
L32	CDR1	Tyr	Tyr	Tyr	Pro	**Tyr**
L34	CDR1	His	His	His	Ala	Glu
L36	FR2	Tyr	Tyr	Tyr	Tyr	Tyr
L49	FR2	Tyr	Tyr	Tyr	Tyr	Tyr
L89	CDR3	Gln	Ser	**Phe**	Gln	Phe
L91	CDR3	Tyr	Val	Ser	Tyr	Gly
L94	CDR3	**Tyr**	Val	Phe	Tyr	Val
L96	CDR3	Leu	Pro	Pro	Leu	Arg
L98	FR4	Phe	Phe	Phe	Phe	Phe
H33	CDR1	Asn	Gly	Gly	Trp	**Tyr**
H35	CDR1	Asn	**Asn**	**Asn**	His	Asn
H37	FR2	Ile	Val	Val	Val	Ala
H47	FR2	Trp	Trp	**Leu**	Trp	Trp
H50	FR2	Asn	Trp	Trp	Met	Phe
H52	FR2	Asp	Asn	Asn	Asp	**Arg**
H53	CDR2	Tyr	Tyr	Tyr	Asn	**Lys**
H93	FR3	Ala	Val	Ala	Thr	Ala
H95	CDR3	Arg	Ala	Gly	**Arg**	Trp
H96	CDR3	Arg	Glu	Thr	–	Gly
H97	CDR3	Asp	Arg	Thr	–	Ser
H98	CDR3	Gly	Leu	Ile	–	–
H100a	CDR3	Tyr	Arg	Arg	–	Tyr
H100b	CDR3	Gly	Thr	Ala	**Asp**	Ala
H100c	CDR3	Phe	Phe	**Met**	**Met**	Met

*Antibodies with a small residue at position H100c, indicated in Table 2a (left), share a binding pocket, as illustrated in Figure 3a. Antibodies with methionine or phenylalanine at position H100c, indicated in Table 2b (right), present a different combining site (Figure 3b). The bottom of the combining site is occupied by TrpH103 in Table 2a and by residue H100c in Table 2b. This table can be compared to Table 2 of MacBeath and Hilvert [3], which concerns esterolytic antibodies. Residue numbering is identical to that of Kabat *et al.* [33], except for the three residues preceding H101, denoted H100a, H100b and H100c, according to Chothia and co-workers [34]. The CDRs consist of residues 26–32, 50–52 and 91–96 for CDRs L1, L2 and L3, respectively, and 26–32, 52–55 and 96–101 for CDRs H1, H2 and H3, respectively. Common residues forming the combining site are indicated in green (residue column); residues essential for catalysis are in bold. Interactions between the antibody and hapten are coloured as follows: cation–π, brown; π-stacking, dark blue; electrostatic, gold; main van der Waals contacts, dark green; direct hydrogen bonding, red; hydrogen-bond network, violet. Residues that are probably implicated in chemical catalysis are shown in cyan. Among the few polar residues of the combining site, H35 is most often involved in the catalytic mechanism. H35 has its sidechain precisely positioned by a conserved hydrogen bond with Trp47. †The only sequence difference at the positions contacting the hapten of the germline antibody is serine at position L34. FR, framework region.

Waals contacts and π-stacking interactions. In addition, a few strategically placed polar functionalities, which modulate the electronic densities on key substituents in the transition state, result in enthalpic stabilisation.

Other strategies

Use of a cofactor

In order to diversify the mechanisms and introduce covalent catalysis, cofactors have been added to the antibody as an alternative to the transition-state analogue approach. The only known structure of a cofactor-dependent antibody catalyst is that of 28B4, which catalyses the periodate-dependent oxidation of sulfide **28** to sulfoxide **29** (Figure 1i) [22]. This reaction was studied as a first step toward extending antibody catalysis to redox reactions. Antibody 28B4 was raised against an aminophosphonic hapten **30** that not only mimics the stereoelectronic features of the transition state, but also contains phosphonate and nitrophenyl moieties designed to provide two binding sites precisely oriented for the substrates periodate and nitroarylsulfide. The antibody stabilises developing positive charge on sulfur and negative charge on periodate in the transition state via cation–π and electrostatic interactions, respectively (Figure 2g). In addition, entropic restriction plays a fundamental role in catalysis through the precise alignment of the thioether substrate and oxidant.

Reactive immunisation

Catalytically active nucleophiles have rarely been selected in antibody combining sites during antibody maturation. In order to improve efficiency and widen the scope of the reactions catalysed, ways have been sought to elicit chemically reactive residues, such as nucleophiles, electrophiles and general bases or acids, directly into the antibody combining site.

Reactive immunisation is based on the use of a chemically reactive hapten designed to irreversibly modify any antibody possessing an active site group that can catalyse the reaction of interest [23]. Antibody 33F12 was obtained using β-diketone hapten **34**, which forms a Schiff base and covalently modifies the ε-amino group of an active site

lysine (Figure 1j) [23]. 33F12 catalyses a vast array of aldol condensations, a C–C bond forming reaction widely utilised in cellular metabolism and synthetic chemistry, as well as retro-aldol reactions. The broad substrate tolerance observed is the result of a lack of maturation of the immune response: because the formation of a covalent bond is the ultimate in achieving binding energy, the binding pocket does not further evolve toward higher specificity. The structure of unliganded antibody 33F12 [24] has confirmed that the framework residue LysH93, which results from a somatic mutation and is essential for catalytic activity [25], is present at the base of the combining site and is probably correctly positioned to act as a nucleophile. LysH93 lies in a hydrophobic environment, so it cannot form any salt bridge or hydrogen bond with the antibody, and is uncharged. This reduces its pK_a and enhances its chemical reactivity.

Strategic use of haptenic charge

Another approach that aims to generate functional residues that could participate in a specific chemical step of catalysis, also termed 'bait and switch' [26–29], uses a hapten containing a charge properly positioned to induce the required complementary charged residue. My colleagues and I recently reported the structure of the complex of antibody 4B2, which catalyses the allylic rearrangement of β–γ unsaturated ketone **35**, with a short derivative of cationic hapten **37** (Figure 1k) [30]. The formation of the dienol intermediate is presumed to occur through abstraction of the Cα proton by a general base, which has been identified as GluL34 on the basis of the structural and biochemical studies. GluL34 forms a direct ionic pair interaction with the amidinium function of **36** (Figure 2h). We emphasised the advantage of the bidentate amidinium group for the precise positioning of a functional group relative to the hapten, compared with quaternary ammoniums, for which the diffuse positive charge is often stabilised by cation–π interactions, as seen in the antibody 5C8–**6** hapten complex (Figure 2b). One might think that introducing a carboxylate moiety into the hapten would, through a similar ionic interaction, induce a positively charged arginine residue in the antibody, which could act as an electrophile or a general acid in a chemical reaction. However, hapten **12** (Figure 1d), which contains two carboxylates, did not select positively charged residues in the combining site of antibody 1F7, which is, moreover, not highly charged. This contrasts with chorismate mutase enzymes, which stabilise the carboxylates of chorismate by a direct ionic pair interaction with arginine residues [13,14]. Other structures of antibodies induced by carboxylate- or amidinium-containing haptens need to be elucidated in order to understand whether the selection of a counter-charged residue is a frequent event or not.

Comparison of the combining site structures

The top of the combining site of antibodies is formed by the CDRs. In particular, CDR loop H3 (H96–H101) is the most heavily used in antibody recognition and has a large diversity potential. Superposition of the coordinates of the catalytic antibodies that possess a small residue at position H100c reveals a common cylindrical cavity, which is also present in hydrolytic antibodies [3,5,31] (Figure 3a). The absence of a bulky residue at position H100c allows deep penetration of the ligands at the V_L–V_H interface and explains the extensive use of framework residues in hapten binding. The common hydrophobic bottom of the cavities is probably a consequence of the similarity and hydrophobicity of the haptens used. The catalytic residues are most often polar residues of CDRs L1, L3, H1 and H3, which make up the walls of the combining site (Table 2a). Fine-tuning of this basic structural motif is achieved through somatic mutation and the diversity inherent to CDR H3.

When a residue with a bulky sidechain (phenylalanine or methionine) is present at position H100c, it fills part of the cavity and makes up the floor of the binding site (Figure 3b). The ligands bind at the upper part of the V_L–V_H interface, leading to a pocket in which the bottom is formed by residues of the CDRs, instead of the framework. This may lead to a combining site that is much shallower than that in Figure 3a, as found in 7G12 (Figure 3b) and 1F7. The positions of the haptens in the combining sites are less similar and the shapes of the cavities are more diversified because the fewer common residues that make up the combining site principally belong to the hypervariable loops (Table 2b).

The importance of residue H100c in determining the shape of the binding cavity suggests that its mutagenesis may confer on the antibodies new catalytic properties.

Conclusions

A comparison of the structures of nonhydrolytic antibody catalysts published during the period 1998 to the present has shown that these antibodies use catalytic pockets of different shapes, depending on the nature of residue H100c. Antibodies with a small or no residue at position H100c present a structurally similar, deep combining site, with hydrophobic residues of the framework making up the floor. When a bulky residue occupies position H100c, it takes up part of the bottom of the cavity; the binding site is formed almost exclusively by the CDRs and adopts various shapes.

The apolar bottom of the combining site of catalytic antibodies serves to exclude the solvent and acts as a template to bind the substrate(s) in a reactive conformation, whereas the more polar residues that form the walls of the cavity play a catalytic role through hydrogen-bonding, cation–π or electrostatic interactions. These pockets are appropriate to govern the regiochemistry and stereochemistry of the reaction, as demonstrated by the control of the fate of intermediates. Moreover, the antibodies often demonstrate stereoselectivity, although no stereochemical information was programmed into the hapten. Hence, antibody catalysts will remain particularly useful to catalyse disfavoured reactions.

Immunological selection based on transition-state analogues results in noncovalent catalysis and narrow substrate specificity. On the other hand, other strategies, such as 'bait and switch' or reactive immunisation, are more appropriate for reactions that necessitate a reactive residue such as a nucleophile or a base/acid. In these new strategies, the hapten does not need to match precisely the transition state of the reaction, but rather generates a functional, strategically positioned residue. This confers on these methods the advantage of generating antibodies with broad substrate tolerance that even catalyse different reactions proceeding through the same mechanism (Table 1). This is especially useful when transition-state analogues are difficult to synthesise, when the structures of the substrate and the transition state are not very different, or when the mechanism of the reaction involves multiple intermediates or transition states.

Improvements in hapten design and screening of antibodies, together with structure-based mutagenesis experiments and random mutagenesis coupled with genetic selection, will, in the future, lead to more efficient antibodies that combine transition-state stabilisation and chemical reactivity.

Update

Antibody 21D8 raised against a 1,5-naphtalene disulfonate hapten catalyses the solvent-sensitive decarboxylation of 3-carboxybenzisoxasoles ($k_{cat}/K_m = 1.1 \times 104\ M^{-1}\ min^{-1}$; $k_{cat} = 57.6\ min^{-1}$; $k_{cat}/k_{non} = 61{,}000$). The antibody-hapten complex structure has recently been determined at 1.61 Å resolution (PDB code 1c5c) [35]. Antibody 21D8 possesses an unusually short H3 loop with no residue at position H100c and presents a combining site illustrated in Figure 3a, with two anionic binding sites for the two sulfonate groups of the hapten. The sidechains of ArgL96 and HisH35 constitute one site, whereas the other is constructed from the sidechains of ArgL46, TrpH103, SerL36 and the backbone amide group of AlaH101. Although the authors computationally docked the substrate and the transition state into 21D8, it was not possible to identify unambiguously in which of the sulfonate-binding sites the carboxylate of the substrate binds. However, one docking mode shows a specific hydrogen bond between the oxygen of the breaking N-O bond and ArgL46 that could stabilise the transition state. Binding throughout the decarboxylation reaction is therefore realised through electrostatic and hydrogen-bonding interactions and by burying the aromatic portion of the substrate in the hydrophobic slot at the bottom of the combining site. Whereas water stabilises the localised charge of the substrate much more than the delocalised charge of the transition state, the antibody is presumed to accelerate the reaction by stabilising the substrate and the transition state to a similar extent, as in aprotic solvents.

Acknowledgements

I thank all my colleagues who read the manuscript: B Badet, B Gigant, J Janin, M Knossow, J-P Mahy and C Tellier.

References

1. Schultz PG, Lerner RA: **From molecular diversity to catalysis: lessons from the immune system.** *Science* 1995, **269**:1835-1842.
2. Blackburn GM, Datta A, Denham H, Wentworth P: **Catalytic antibodies.** *Adv Phys Org Chem* 1998, **31**:249-392.
3. MacBeath G, Hilvert D: **Hydrolytic antibodies: variation on a theme.** *Chem Biol* 1996, **3**:433-445.
4. Wade H, Scanlan TS: **The structural and functional basis of antibody catalysis.** *Annu Rev Biophys Biomol Struct* 1997, **26**:461-493.
5. Charbonnier J-B, Gigant B, Golinelli-Pimpaneau B, Knossow M: **Similarities of hydrolytic antibodies revealed by their X-ray structures: a review.** *Biochimie* 1997, **79**:653-660.
6. Hilvert D, MacBeath G, Shin JA: **The structural basis of antibody catalysis.** In *Bioorganic Chemistry: Peptides and Proteins*. Edited by Hecht SM. New York: Oxford University Press; 1998:355-366.
7. Romesberg FE, Santarsiero BD, Spiller B, Yin J, Barnes D, Schultz PG, Stevens RC: **Structural and kinetic evidence for strain in biological catalysis.** *Biochemistry* 1998, **37**:14404-14409.
8. Gruber K, Zhou B, Houk KN, Lerner RA, Shevlin CG, Wilson IA: **Structural basis for antibody catalysis of a disfavored ring closure reaction.** *Biochemistry* 1999, **38**:7062-7074.
9. Li T, Lerner RA, Janda KD: **Antibody-catalyzed cationic reactions: rerouting of chemical transformations via antibody catalysis.** *Acc Chem Res* 1997, **30**:115-121.
10. Paschall CM, Hasserodt J, Jones T, Lerner RA, Janda KD, Christianson DW: **Convergence of catalytic antibody and terpene cyclase mechanisms : polyene cyclisation directed by carbocation-π interactions.** *Angew Chem Int Ed Engl* 1999, **38**:1743-1747.
11. Laschat S: **Pericyclic reactions in biological systems. Does Nature know about the Diels-Alder reaction?** *Angew Chem Int Ed Engl* 1996, **35**:289-291.
12. Haynes MR, Stura EA, Hilvert D, Wilson IA: **Routes to catalysis: structure of a catalytic antibody and comparison with its natural counterpart.** *Science* 1994, **263**:646-652.
13. Chook YM, Hengming K, Lipscomb WN: **Crystal structures of the monofunctional chorismate mutase from *Bacillus subtilis* and its complex with a transition state analog.** *Proc Natl Acad Sci USA* 1993, **90**:8600-8603.
14. Lee AY, Karplus PA, Ganem B, Clardy J: **Atomic structure of the buried catalytic pocket of *Escherichia coli* chorismate mutase.** *J Am Chem Soc* 1995, **117**:3627-3628.
15. Ulrich HD, Mundorff E, Santarsiero BD, Driggers EM, Stevens RC, Schultz PG: **The interplay between binding energy and catalysis in the evolution of a catalytic antibody.** *Nature* 1997, **389**:271-274.
16. Mundorff EC, Hansin MA, Varvak A, Ulrich H, Schultz PG, Stevens RC: **Conformational effects in biological catalysis: an antibody-catalyzed oxy-Cope rearrangement.** *Biochemistry* 2000, **39**:627-632.
17. Romesberg FE, Spiller B, Schultz PG, Stevens RC: **Immunological origins of binding and catalysis in a Diels-alderase antibody.** *Science* 1998, **279**:1929-1933.
18. Heine A, Stura EA, Yli-Kauhaluoma JT, Gao C, Deng Q, Beno BR, Houk KN, Janda KD, Wilson IA: **An antibody *exo* Diels-alderase inhibitor complex at 1.95 Angstrom resolution.** *Science* 1998, **279**:1934-1940.
19. Xu J, Deng Q, Chen J, Houk KN, Bartek J, Hilvert D, Wilson IA: **Evolution of shape complementarity and catalytic efficiency from a primordial antibody template.** *Science* 1999, **286**:2345-2348.
20. Campbell AP, Tarasow TM, Massefski W, Wright PE, Hilvert D: **Binding of a high-energy substrate conformer in antibody catalysis.** *Proc Natl Acad Sci USA* 1993, **99**:8663-8667.
21. Driggers EM, Cho HS, Liu CW, Katzka CP, Braisted AC, Ulrich HD, Wemmer DE, Schultz PG: **Mechanistic studies of an antibody-catalyzed pericyclic rearrangement.** *J Am Chem Soc* 1998, **120**:1945-1958.

22. Hsieh-Wilson LC, Schultz PG, Stevens RC: **Insights into antibody catalysis: structure of an oxygenation catalyst at 1.9 Å resolution.** *Proc Natl Acad Sci USA* 1996, **93**:5363-5367.

23. Wagner J, Lerner RA, Barbas CF III: **Efficient aldolase catalytic antibodies that use the enamine mechanism of natural enzymes.** *Science* 1995, **270**:1797-1800.

24. Barbas CF III, Heine A, Zhong G, Hoffman T, Gramatikova S, Björnestedt R, List B, Anderson J, Stura EA, Wilson IA, Lerner RA: **Immune versus natural selection: antibody aldolases with enzymic rates but broader scope.** *Science* 1997, **278**:2085-2092.

25. Karlstrom A, Zhong G, Rader C, Larsen NA, Heine A, Fuller R, List B, Tanaka F, Wilson IA, Barbas CF III, Lerner RA: **Using antibody catalysis to study the outcome of multiple evolutionary trials of a chemical task.** *Proc Natl Acad Sci USA* 2000, **97**:3878-3883.

26. Shokat KM, Leumann CJ, Sugasawara R, Schultz PG: **A new strategy for the generation of catalytic antibodies.** *Nature* 1989, **338**:269-271.

27. Janda KD, Weinhouse MI, Schloeder DM, Lerner RA, Benkovic SJ: **Bait and switch strategy for obtaining catalytic antibodies with acyl-transfer capabilities.** *J Am Chem Soc* 1990, **112**:1274-1275.

28. Janda KD, Weinhouse MI, Danon T, Pacelli KA, Schloeder DM: **Antibody bait and switch catalysis: a survey of antigens capable of inducing abzymes with acyl-transfer properties.** *J Am Chem Soc* 1991, **113**:5427-5434.

29. Thorn SN, Daniels RG, Auditor MT, Hilvert D: **Large accelerations in antibody catalysis by strategic use of haptenic charge.** *Nature* 1995, **373**:228-230.

30. Golinelli-Pimpaneau B, Gonçalves O, Dintinger T, Blanchard D, Knossow M, Tellier C: **Structural evidence for a programmed general base in the active site of a catalytic antibody.** *Proc Natl Acad Sci USA* 2000, **97**:9892-9895.

31. Charbonnier J-B, Carpenter E, Gigant B, Golinelli-Pimpaneau B, Tawfik D, Eshhar Z, Green BS, Knossow M: **Crystal structure of the complex of a catalytic antibody Fab fragment with a transition state analog: structural similarities in esterase-like catalytic antibodies.** *Proc Natl Acad Sci USA* 1995, **92**:11721-11725.

32. Gigant B, Tsumuraya T, Fujii I, Knossow M: **Diverse structural solutions to catalysis in a family of antibodies.** *Structure* 1999, **7**:1385-1393.

33. Kabat EA, Wu TT, Perry HM, Gottesman KS, Foeller C: *Sequences of Proteins of Immunological Interest*. Bethesda, MD: US Public Health Service, National Institutes of Health; 1991.

34. Morea V, Tramontano A, Rustici M, Chothia C, Lesk AM: **Conformations of the third hypervariable region in the V_H domain of immunoglobulins.** *J Mol Biol* 1998, **257**:269-294.

35. Hotta K, Lange H, Tantillo DJ, Houk KN, Hilvert D, Wilson IA : **Catalysis of decarboxylation by a preorganized heterogeneous microenvironment: crystal structures of abzyme 21D8.** *J Mol Biol* 2000, **302**:1213-1225.